The systemin signaling cascade as derived from phosphorylation time courses under stimulation by systemin and its inactive Thr17Ala (A17) analog

Fatima Haj Ahmad, Xuna Wu, Annick Stintzi, Andreas Schaller, Waltraud X Schulze

University of Hohenheim, Institute of Plant Physiology and Biotechnology, 70593 Stuttgart, Germany

Abstract

Systemin is a small peptide with important functions in plant wound response signaling. Although transcriptional responses of systemin action are well described, the precise signaling cascades involved in its perception and signal transduction are poorly understood at the protein level. Here we use a phosphoproteomic profiling study involving stimulation time courses with systemin and its inactive analogon A17 to reconstruct a systemin-specific kinase/phosphatase signaling network. The time course analysis of systemin-induced phosphorylation patterns revealed early events at the plasma membrane, such dephosphorylation of H^+-ATPase, rapid phosphorylation of NADPH-oxidase and Ca^{2+}-ATPase. Later responses involved transient phosphorylation of small GTPases and vesicle trafficking proteins, as well as transcription factors. Based on a correlation analysis of systemin-specific phosphorylation profiles, we predict substrate candidates for 56 systemin specific kinases and 18 phosphatases. Among the kinases are several systemin-specific receptor kinases as well as kinases with downstream signaling functions, such as MAP-kinases. A regulatory circuit for plasma membrane H^+-ATPase was predicted and confirmed by in-vitro activity assays. In this regulatory model we propose that upon systemin treatment, H^+-ATPase LHA1 is rapidly de-phosphorylated at its C-terminal regulatory residue T955 by phosphatase PLL5, resulting in the alkalization of the growth medium within 2 minutes of systemin treatment. We further propose that the H^+-ATPase LHA1 is re-activated by MAP-Kinase MPK2 later in the systemin response. MPK2 was identified with increased phosphorylation at its activating TEY-motif at 15 minutes of treatment and the predicted interaction with LHA1 was confirmed by in-vitro kinase assays. Our data set provides a valuable resource of proteomic events involved in the systemin signaling cascade with a focus on predictions of substrates to systemin-specific kinases and phosphatases.

Key words: Systemin signaling specificity, phosphoproteomics, plasma membrane, Solanum lycopersicum

Introduction

Almost 30 years ago, the quest for signaling molecules mediating systemic defense responses after local injury by insect herbivores culminated in the discovery of systemin as the first peptide with signaling function in plants (1, 2). The 18-amino-acid oligopeptide was established as an essential component of the wound signaling pathway that is responsible for the systemic regulation of defense gene expression (3, 4). Systemin was initially described as the long-sought hormonal signal that is released at the site of wounding, that travels through the vasculature and induces the defense response in distal, unwounded tissues (2, 5). However, this model had to be modified when it was shown that systemin rather acts locally at the site of wounding, where it induces and amplifies the production of jasmonates as systemic signals for defense gene activation in distal tissues (6, 7). Considering its paracrine immune-modulatory activity, systemin is thus better described as a plant cytokine, a phytocytokine (8) rather than a wound hormone. Systemin is synthesized as a larger precursor protein from which it is proteolytically released (4, 9). Whether or not precursor processing and systemin secretion are regulated processes still awaits an answer. On the other hand, if systemin is released passively simply as a result of tissue disruption, it could also be addressed as a damage-associated molecular pattern, a DAMP (8).

Local action of systemin is initiated by its interaction with a saturatable binding site at the cell surface (10, 11). Purification and characterization of the binding protein tentatively placed the receptor into the family of leucin-rich repeat receptor-like kinases (LRR-RLKs), but the protein initially declared as the systemin receptor later turned out to be the tomato ortholog of BRI1, the brassinosteroid receptor in Arabidopsis (12-15). Recent work identified the systemin receptor as SR470, a LRR-RLK closely related to known pattern recognition receptors (16). The early cellular responses to systemin do in fact resemble those typically triggered by microbe-associated molecular patterns (MAMPs) including an increase in cytosolic calcium, extracellular alkalization, plasma membrane depolarization, an oxidative burst, and ethylene production (17-19). By still unknown mechanisms, these early signaling events translate into the activation of the octadecanoid pathway for jasmonate production (20-22). The locally produced jasmonate signal is then perceived in distal leaves resulting in the systemic activation of defense responses (23). In addition to the slow-moving jasmonate signal, rapidly propagating electrical and calcium signals have been linked to the activation of jasmonate signaling and activation of wound response gene expression in systemic tissues (24-26).

Despite almost 30 years of research, it is still unclear how early responses at the plasma membrane are activated by systemin, and how these early signaling events including the influx of calcium, plasma membrane depolarization, and the production of reactive oxygen species are linked to downsteam events, like jasmonate production and defense gene activation. Since systemin is perceived by a receptor kinase, it is reasonable to assume that subsequent events are regulated by phosphorylation and can thus be captured by phosphoproteomics. Large scale phosphoproteomics was shown to be a powerful tool to identify global patterns and novel players in plant signaling networks. For example, time-courses studies of phosphorylation patterns in response to sucrose (27) has led to the identification of a novel kinase, SIRK1, regulating aquaporins (28). The cellular response to nitrate was well studied by large-scale phosphoproteomics to conclude about the cellular kinase network involved (29). Also for plant hormones, such as brassinolide, large-scale phosphoproteomics time-course studies revealed novel insights into the intracellular signaling network (30). Phosphoproteomics resulted in the identification of FERONIA as the receptor of rapid alkalization factor, and the plasma membrane H^+-ATPase as a downstream target (31). In a similar approach, we used time-resolved phosphoproteomics in a systemin-responsive cell culture system to get further insight into the systemin signaling cascade and the sequence of early signaling events.

Experimental procedures

Experimental Design and statistical rationale

Cell suspension cultures of *Solanum peruvianum* (200 ml) were subjected to stimulation with 10 nM systemin (sys), 10 nM of the inactive Thr17Ala analog (A17), or injected with equal volume (1 ml) of water (w). For each treatment, a batch of cells was harvested after 2, 5, 15 and 45 minutes (Figure 1A). Untreated cells were harvested as controls at time point 0. All treatments and time points were sampled from three independent replicates using independent batches of cells in each experiment. Data analysis was carried out jointly for all samples by averaging quantitative information for each time point and treatment across the three replicates. The same cell culture materials were used for phosphoproteome profiling as well as for activity assay. For phosphopeptide profiling, microsomal membranes were isolated from each sample, digested with trypsin, enriched for phosphopeptides and subjected to untargeted data-dependent acquisition by LC-MS/MS.

Cell suspension cultures and alkalization assay

The *Solanum peruvianum* cell suspension culture was kindly provided by Georg Felix (University of Tübingen). Cells were subcultured weekly by diluting 8 ml of the suspension in 70 ml fresh Murashige-Skoog medium containing Nitsch vitamins (32), 0.34 g/l KH_2PO_4, 5 mg/l 1-naphthaleneacetic acid and 2 mg/l benzylaminopurine and grown on a rotary shaker at 26 °C with 120 rpm. For the alkalization assay continuous measurements of extracellular pH was performed in 10 ml of cultured cells 6–8 days after subculture. Synthetic systemin and systemin-A17 peptides (Pepmic; Suzhou, China) were added from a 200-fold concentrated stock solution in water.

Microsomal fraction extraction

The microsomal fraction was extracted according to (33) with minor modifications. A total of 1 g of harvested cells was homogenized in 10 ml extraction buffer (330 mM sucrose, 100 mM KCl, 1 mM EDTA, 50 mM Tris-MES pH 7.5 and fresh 5 mM DTT) in the presence of 1 % v/v proteinase inhibitor mixture (Serva) and 0.5 % of each phosphatase inhibitor cocktails 2 & 3 (Sigma-Aldrich, Germany) in a Dounce Homogenizer. At least 200 strokes were performed. The homogenate was filtered through four layers of miracloth and centrifuged for 15 min at 7500 × g at 4 °C. The supernatant was collected and centrifuged for 75 min at 48,000 × g at 4 °C. The pellet was washed with 5 ml of 100 mM Na_2CO_3 then again was centrifuged for 75 min at 48,000 x g at 4 °C. The microsomal membrane pellets used for LC-MS/MS were re-suspended in 100 µl UTU (6 M urea, 2 M thiourea and 10 mM Tris-HCl pH 8). Microsomal membrane pellets used for ATPase assay were re-suspended in 100 µl of re-suspension buffer (330 mM sucrose, 25 mM Tris-MES pH 7.5, 0.5 mM DTT). Protein concentrations were determined using Bradford assay (Roth, Germany) with BSA as protein standard. Samples were stored at −80 °C until further use.

Protein preparation for LC-MS/MS

Microsomal proteins were predigested for three hours with endoproteinase Lys-C (0.5 µg/µl; Thermo Scientific) at 37 °C. After 4-fold dilution with 10 mM Tris-HCl (pH 8), samples were digested with 4 µL Sequencing Grade Modified trypsin (0.5 µg/µl; GE Life Sciences) overnight at 37 °C. The reaction was stopped by addition of trifluoroacetic acid (TFA) to reach pH $\leqslant$ 3 before further processing.

Phosphopeptide enrichment

Phosphopeptides were enriched over titanium dioxide (TiO_2, GL Sciences) with some modifications as described (34). TiO_2 beads were equilibrated with 100 µl of 1 M glycolic acid, 80% acetonitrile and 5 % TFA. The digested peptides were mixed with the same volume of the equilibration solution and

incubated for 20 minutes with 2 mg TiO_2 beads with continuous shaking. After brief centrifugation, the supernatant was discarded and the beads were washed 3 times with 80 % acetonitrile and 1% TFA. Then the phosphopeptides were eluted with 240 µl of 1% ammonium hydroxide. Eluates were immediately acidified by adding 50 µl 10% formic acid to reach pH<3. Enriched phosphopeptides were desalted over C18-Stage tip (35) prior to mass spectrometric analysis.

LC-MS/MS analysis of peptides and phosphopeptides

Tryptic peptide mixtures were analyzed by LC/MS/MS using nanoflow Easy-nLC1000 (Thermo Scientific) as an HPLC-system and a Quadrupole-Orbitrap hybrid mass spectrometer (Q-Exactive Plus, Thermo Scientific) as a mass analyzer. Peptides were eluted from a 75 µm x 50 cm C18 analytical column (PepMan, Thermo Scientific) on a linear gradient running from 4 to 64% acetonitrile in 240 min and sprayed directly into the Q-Exactive mass spectrometer. Proteins were identified by MS/MS using information-dependent acquisition of fragmentation spectra of multiple charged peptides. Up to twelve data-dependent MS/MS spectra were acquired for each full-scan spectrum recorded at 70,000 full-width half-maximum resolution. Fragment spectra were acquired at a resolution of 35,000. Overall cycle time was approximately one second.

Protein identification and ion intensity quantitation was carried out by MaxQuant version 1.5.3.8 (36). Spectra were matched against the Tomato proteome (Solanum lycopersicum, ITAG2.4, 34725 entries) using Andromeda (37). Thereby, carbamidomethylation of cysteine was set as a fixed modification; oxidation of methionine as well as phosphorylation of serine, threonine and tyrosine was set as variable modifications. Mass tolerance for the database search was set to 20 ppm on full scans and 0.5 Da for fragment ions. Multiplicity was set to 1. For label-free quantitation, retention time matching between runs was chosen within a time window of two minutes. Peptide false discovery rate (FDR) and protein FDR were set to 0.01, while site FDR was set to 0.05. Hits to contaminants (e.g. keratins) and reverse hits identified by MaxQuant were excluded from further analysis. Raw files and identified spectra were submitted to ProteomeXChange and are available to the public under the accession number PXD010819.

Mass spectrometric data analysis and statistics

Reported ion intensity values were used for quantitative data analysis. cRacker (38) was used for label-free data analysis of phosphopeptide ion intensities based on the MaxQuant output (evidence.txt). All phosphopeptides and proteotypic non-phosphopeptides were used for quantitation. Within each sample, ion intensities of each peptide ions species (each m/z) were normalized against the total ion intensities in that sample (peptide ion intensity/total sum of ion intensities). Subsequently, each peptide ion species (i.e. each m/z value) was scaled against the average normalized intensities of that ion across all treatments. For each peptide, values from three biological replicates then were averaged after normalization and scaling. In case of non-phosphopeptides, protein ion intensity sums were calculated from normalized scan scaled ion intensities of all proteotypic peptides. A list of quantified phosphopeptides including normalized ion intensities, standard deviation and number of spectra is available as Supplementary Table 1.

H^+-ATPase activity assay

Plasma membrane (PM) H^+-ATPase activity was determined by resuspending 5 µg of microsomal proteins in 10µl resuspension buffer and 40 µl of reaction buffer containing 25 mM Tris-HCl pH 6.3, 50 mM KCl, 5 mM $MgCl_2$, 5 mM $CaCl_2$, 0.1 mM Ouabain (Thermo Fisher Scientific, USA), 1 mM NaN_3, 100 nM Concanamycin A (Sigma-Aldrich, Germany), 0.02 % Brij58 (Sigma-Aldrich, Germany), 0.5 µg/µl BSA and 10 mM DTT. The reaction was initiated by the addition of 1 mM ATP, proceeded for 2 hours at room temperature, and stopped with 150 µl of stopping reagent (8% ascorbic acid, 2.1% HCl

and 0.7% ammonium molybdate). After 5 min, 150 µl of 2% tri-sodium citrate and 2% acetic acid solution was added and incubated for 15 min at room temperature. The absorbance as a measure of inorganic phosphate was measured at 640 nm using plate reader (Tecan Spark). ATPase activity was measured with and without 400 µM orthovanadate (Na_3VO_4), and the difference between these two activities was attributed to the PM H^+-ATPase.

Recombinant protein expression

The whole coding sequence of MPK2 (Solyc08g014420.2.1) was amplified by PCR using the primers ATTACCATGGCAGATGGTTCAGCTCCG (forward) and ATATCTCGAGCATGTGCTGGTATTCGGGATT (reverse) with *S. lycopersicum* leaf cDNA as template. The PCR product was cloned into pCR2.1-TOPO vector (Thermo Scientific) and amplified in *E. coli*. The MPK2 insert was excised with *NcoI* and *XhoI* (underlined in the primer sequence) and ligated to pET21d (+) (Merck; Darmstadt, Germany) to produce 14420HispET21d, which was transformed into *E.coli* strain BL21 RIL (Agilent Technologies; Waldbronn, Germany) to be expressed as C-terminally 6xHis-tagged recombinant protein. MPK2 was expressed in unmodified form and as constitutively active mutant (CA) with two amino acid substitutions D216G/E220A (39).

The mutations were introduced using the following primers: ATTACCATGGCAGATGGTTCAGCTCCG and 14420D216G/E220AR1 (GTCACAACATATGCGGTCATAAAGCCAGTTTCAGAAG); or 14420D216G/E220AF2 (CTTCTGAAACTGGCTTTATGACCGCATATGTTGTGAC) and (ATATCTCGAGCATGTGCTGGTATTCGGGATT).

For PLL5 (Solyc06g076100.2.1), the catalytic domain (residues from 241-708) was amplified by PCR using the primers ATACCATGGCACATCACCATCACCATCACTTCAGCAGTGAGTGTAGTTTG and AATTCTCGAGTTATGCACTGGATCTCCATATTC.

The PCR products were cloned into pET21d (+) as described above to produce His76100pET21d, which was transformed into *E.coli* strain BL21 RIL to be expressed as N-terminally 6xHis-tagged recombinant protein.

Purification of His-tagged proteins

E.coli BL21 RIL cells were grown at 37 °C , 200 rpm to an A_{600} value of 0.8 and then induced with 1 mM isopropyl-β -d-thiogalactopyranoside (IPTG) for 4 h at 30 °C. Cells were pelleted by centrifugation and lysed in Bugbuster™ protein extraction reagent (Merck; Darmstadt, Germany) by continuous agitation for 20 min at room temperature. After centrifugation at 12,000 g for 20 min at 4 °C, the supernatants were collected. The supernatants were subjected to affinity purification on Ni-NTA agarose following the manufacturer's instructions (Qiagen; Hilden, Germany).

In-vitro kinase activity assay

Recombinant MPK2 (2 µg) was incubated with peptide substrate (GLDIETIQQSYTV; amount as indicated for each experiment) overnight in 50 µl of reaction buffer (20 mM HEPES pH 7.0, 10 mM $MgCl_2$, 2 mM DTT and 0.1 mg/ml BSA) with 1 µM ATP at 30 °C. Kinase activity was measured as ATP consumption by addition of 50 µl of Kinase-Glo® Plus Reagents (Promega; Fitchburg, WI), 10 min incubation at 30°C, and subsequent recording of the decrease in luminescence (Tecan Spark luminometer). To detect the phosphorylated peptides by mass spectrometry, the reaction was performed as described with 20 µg of peptide substrate. The reaction was stopped by addition of TFA until pH $\leqslant$ 3 and reaction products were purified over C18-Stage tips (35) prior to mass spectrometric analysis.

In-vitro phosphatase activity assay

Recombinant PLL5 phosphatase (1 µg) was incubated with the phosphorylated peptide substrate (GLDIETIQQSYT(ph)V; amount as indicated for each experiment) in 50 µl of reaction buffer (20 mM Tris-HCl pH 7.5, 5 mM $MgCl_2$, 1mM EGTA, 0.02 % β-mercaptoethanol and 0.1 mg/ml BSA) at room temperature for 30 minutes. Released phosphate was detected by addition of 150 µl of 8 % ascorbic acid, 2.1 % HCl and 0.7 % ammonium molybdate. After 5 min at room temperature the reaction was stopped by addition of 150 µl 2 % tri-sodium citrate and 2 % acetic acid (40). After incubation for 15 min at room temperature the reduced phoshomolybdenum complex was quantified at 640 nm using a plate reader (Tecan Spark) based on a standard curve of 0 - 0.1µmol K2HPO4. To detect the unphosphorylated peptides by mass spectrometry, the reaction was performed as above with 200 µg of phosphorylated peptide substrate. The reaction was stopped by addition of TFA to reach pH $\leqslant$ 3 and reaction products were purified over C18-Stage tips (4) prior to mass spectrometric analysis.

Results

The inactive A17 systemin analogon allows definition of systemin specificity

Early cellular responses to systemin include a rapid influx of calcium and depolarization of the plasma membrane which are necessary and sufficient for systemin signaling and induction of the wound response (17-19, 41, 42). Systemin-induced changes in plasma membrane ion permeability can be assayed conveniently in tomato (*Solanum peruvianum*) cell cultures as an alkalization of the culture medium (18) (Figure 2A). This cell culture system was used here to analyze dynamic changes of protein phosphorylation in the systemin signaling network.

Systemin responses, including extracellular alkalization, the induction of ethylene biosynthesis, and expression of wound response genes are inhibited by A17, a systemin derivative in which the penultimate threonine residue is substituted by alanine (18, 43, 44). In our cell culture system, stimulation with 10 nM systemin resulted in a rapid alkalization of the medium from pH 5.5 to pH 6.4 within about 8 minutes (Figure 2A). A17 was completely inactive at this concentration. When A17 was added to the systemin treatment, the alkalization response was reduced with increasing concentrations of A17 (Figure 2B). To explain the antagonistic activity of A17, it was suggested that the peptide may interact with the binding site of the systemin perception system (43). Consistent with this proposition, binding to the putative receptor was shown to rely on the N-terminus of systemin, while the C-terminus, including Thr17, is required for activation (10). The receptor was recently identified as SYR1, and A17 was confirmed as a competitive systemin antagonist (16). By comparing phosphoproteomic responses triggered by A17 and by systemin, we will be able to filter the data set for systemin-specific phosphorylation changes. We therefore included the inactive A17 analog as a control in our experiments.

Description of the phosphoproteomics data set

A total of 3312 phosphopeptide species were identified. Most of the identified phosphopeptides were singly phosphorylated and 89.5% of identified phosphorylation sites were phosphoserines (Figure 1 B, C). Quantitative information under at least one treatment condition was obtained for 2960 phosphopeptide species matching 1309 protein models in at least one biological replicate. Thereby, the majority of phosphopeptides were identified at all time points (Figure 3A). The high overlap of identified phosphopeptides across the time course indicates high analytical reproducibility and high potential for good quantitative coverage. At each sampled time point, the majority of phosphopeptides was identified under all treatment conditions (Figure 3B). However, at 5 minutes, 15 minutes and 45 minutes, a large number of phosphopeptides was identified only after systemin stimulation. Far fewer phosphopeptides were found to be specific for the A17 or water control treatments.

Phosphorylation time profiles

Treatment of suspension cell cultures with systemin resulted in characteristic changes of phosphorylation patterns. K-means clustering was used to group these phosphorylation responses (Figure 4A; Supplementary Table 2). A high number of 827 phosphopeptides was rapidly dephosphorylated upon systemin treatment (cluster A). Three clusters were characterized by a transient increase in phosphorylation, with 465 phosphopeptides peaking at 2 minutes (cluster B), 501 at 5 minutes (cluster C), and 705 at 15 minutes after systemin treatment (cluster D). Further 1001 phosphopeptides were classified as not responsive (cluster F). The stimulation of suspension cells with A17 also resulted in characteristic changes in phosphorylation (Figure 4B). Interestingly, upon A17 stimulation no phosphopeptides displayed a transient increase in phosphorylation at 5 minutes, i.e. cluster C is missing. Instead, 1042 phosphopeptides showed an increase in phosphorylation at 45 minutes (cluster E). This response was not observed upon systemin treatment. Stimulation of the suspension cells with water resulted in response groups very similar to the clusters observed upon A17 treatment (Figure 4C). Particularly, cluster C with a phosphorylation peak at 5 minutes also was missing, and cluster E with maximum phosphorylation at 45 minutes was observed. The missing cluster C and emergence of a "later" maximum in cluster E in both A17 treatment and water stimulation suggests that the control treatments A17 and water do trigger some cellular response, but weaker and delayed compared to systemin treatment.

To substantiate the observed phosphorylation profiles as physiologically relevant, we analyzed the activity of the plasma membrane H^+-ATPase (Figure 5) that has previously been implicated in the systemin-induced alkalization response (19). Two phosphopeptides of the C-terminal regulatory domain of plasma membrane ATPases Solyc07g017780 (AHA1) and Solyc03g113400 (LHA1) were identified with different time profiles under all three treatments. The peptides encompass the penultimate threonine residue, phosphorylation of which facilitates 14-3-3 protein binding and proton pump activation (45, 46). In agreement with the observed alkalization of the growth medium upon systemin treatment, the peptides were slightly dephosphorylated at 2 minutes of treatment (Figure 5 A, B). Dephosphorylation of the regulatory threonine residue was associated indeed with a measureable decrease in H^+-ATPase activity at 2 to 5 minutes of systemin treatment (Figure 5C). In contrast, A17 and water treatment induced a very transient increase in C-terminal phosphorylation and H^+-ATPase activity at 2 minutes. We conclude that the time profiles presented in Figure 4 present precise quantitative measurements of phosphorylation status with corresponding effects on protein activity.

Processes involved in the systemin response

To better understand the processes at each time point, we carried out an over-representation analysis (Fisher Exact Test) of the phosphoproteins present in each of the clusters A to F under systemin stimulation (Figure 6A). Proteins with functions in signaling (MapMan bin 30; p-value < 3.7E-19), transport (bin 34; p-value <2.3E-24), cellular processes (bin 31; p-value <3.0E-16), RNA related processes (bin 27; p-value <8.4E-6), and cell wall proteins (bin 10; p-value <3.9E-5) were highly over-represented in several clusters (Supplementary Table 3). Furthermore, several phosphopeptides were identified which were annotated as being involved in stress (bin 20), protein-related responses (bin 29) and hormone signaling (bin 17).

The abundance distribution of proteins in different MapMan subbins revealed cluster-specific distributions: cellulose synthesis proteins (bin 10.2) and proteins involved in auxin signaling (bin 17.2.3) were most abundant in cluster B (2 min). Proteins related to biotic stress (bin 20.1), calcium signaling (bin 30.3) and protein degradation (bin 29.5) were most abundant in cluster C (5 min). P- and V-type ATPases (bin 34.1) and signaling G-proteins (bin 30.5) were most abundant in cluster D

(15 min). Vesicle transport proteins (bin 31.4) were highly abundant in clusters B and C, while transcription factors (bin 27.3) and protein post-translational modification (bin 29.4) were abundant in all clusters.

Systemin-specific responses

To define precisely which of the phosphorylation events are systemin-specific, we compared for each phosphopeptide the phosphorylation time profile induced by systemin with those induced by A17 or water (Figure 6B). For example, 649 out of 727 phosphopeptides in systemin-induced cluster A (de-phosphorylated after 2 min), were classified in a "later" cluster (B to F) upon A17 treatment, or were not identified at all (7 phosphopeptides). Thus, these proteins were considered systemin-specific. Only 71 phosphopeptides showed the same rapid de-phosphorylation kinetics (i.e. also classified as cluster A) when treated with A17. In contrast, 665 of the 1001 phosphopeptides that were clustered as non-responsive to systemin treatment (cluster F), upon A17 treatment showed a peak phosphorylation in an earlier cluster. A total of 161 proteins were found with equal classification upon A17 and systemin treatment, and 83 phosphopeptides were not identified in the A17 treatment. In total, 1515 phosphopeptides (45% of all identified phosphopeptides) were classified as systemin-specific.

Based on this classification, most phosphopeptides with transient systemin-induced phosphorylation change displayed a delayed response upon A17 stimulation, if any. The phosphopeptides not identified upon A17 treatment were particularly enriched for vesicle transport proteins (bin 31.4), cellulose synthases (bin 10.2), P- and V-ATPases (bin 34.1), and auxin-related processes (bin 17.2.3) (Supplementary Table 4). Among the systemin-specific phosphopeptides, 105 and 18 phosphopeptides matched 78 protein kinases and 18 phosphatases, respectively (Supplementary Table 5).

Not all phosphopeptides from the 78 systemin-specific kinases met the requirement of at least four quantitative values across the time course and were therefore excluded from further analysis. The phosphorylation profiles of the peptides from the remaining 56 kinases and the 18 phosphatase-derived peptides were then used to construct a correlation network of systemin-specific responses. Each phosphopeptide of a kinase or phosphatase was correlated against all other phosphopeptides from the functional categories over-represented in the systemin-induced response clusters (Figure 6A). A stringent cutoff-value of r=0.85 was used to display individual proteins connected by the systemin-specific kinases or phosphatases (Figure 7A, B). For each kinase/phosphatase in the networks, node size reflects its degree, i.e. the number of interacting target proteins. Specifically, for the proteins in cluster A with fast dephosphorylation response, phosphopeptides from a MAP-triple kinase (S(ph)SNATVEASGLSR, Solyc11g033270), a protein phosphatase 1 regulatory subunit (LSS(ph)PAAQS(ph)PSVSTK, Solyc02g070260) and a protein phosphatase C (LTNS(ph)PDVEIK, Solyc10g005640) had the highest degree in the correlation network (210, 134, 118 respectively). These proteins had highest numbers of systemin-specific correlation partners. Other kinases with high degree (number of interactions) were an uncharacterized kinase family protein (AIS(ph)LPS(ph)SPR, Solyc02g076780, degree 118), a calcium-dependent protein kinase (CDPK)-related kinase (TES(ph)GIFR, Solyc10g078390, degree 115), and a receptor like kinase (S(ph)FENEIR, Solyc09g072810, degree 110). Among proteins displaying transient phosphorylation at 2 minutes (cluster B) we found CBL-interacting protein kinase (T(ph)TCGTPNYVAPEVLSHK, Solyc04g076810, degree 112), serine/threonine protein kinase (NQGS(ph)PSDTCSESDHK, Solyc01g108920, degree 110) and cell division protein kinase (DRLDS(ph)IDGK, Solyc07g063130, degree 102) with highest degrees. For proteins with transient phosphorylation at 5 minutes (cluster C), the protein kinases with highest degree were the ethylene receptor (GGS(ph)QTDSSISTSHFGGK, Solyc05g055070, degree 103), and two receptor kinases (SIDLFTDVSEEGLS(ph)PR, Solyc09g083210, degree 49;

ENPGDS(ph)GSLVQPGHDIEK, Solyc12g010740, degree 44). Kinases with highest degree among the proteins with transient phosphorylation at 15 minutes (cluster D) were a serine/threonine protein kinase (SEEVDGS(ph)SSIR, Solyc11g033270, degree 210), the activating motif of a mitogen activated protein kinase (VTSETDFM(ox)T(ph)EY(ph)VVTR, Solyc08g014420, degree 128), and a uncharacterized protein kinase (S(ph)AAGTPEWM(ox)APEVLR, Solyc09g009090, degree 122).

Interestingly, these protein kinases with high degree often were identified with several phosphorylation sites which showed different response profiles during the systemin treatment. For example, the MAP-triple kinase (MAPKKK) Solyc11g033270 (degree 210) was identified with two phosphorylation sites outside the kinase domain: S(ph)SNATVEASGLSR (Ser859) showed rapid dephosphorylation (cluster A) and SEEVDGS(ph)SSIR (Ser345) showed transient phosphorylation at 15 minutes (cluster D).

Time profile of the rapidly dephosphorylated MAPKKK peptide S(ph)SNATVEASGLSR showed highest correlation with dephosphorylated peptides of an ubiquitin ligase (LEEGS(ph)SPEQR, Solyc05g007820), a YAK1 homologous protein kinase (TVYSY(ph)IQSR, Solyc03g097350) and a RNA recognition motif containing protein (SSDS(ph)QELTTTELK, Solyc02g062290), and a protein phosphatase 2C family protein (LTSS(ph)PEAEIK, Solyc06g065580). The finding that kinases and phosphatases correlate with the same phosphopeptide suggest kinase-phosphatase activation/inactivation loops upon systemin stimulation. At 15 minutes of systemin treatment, the MAPKKK phosphopeptide SEEVDGS(ph)SSIR of protein kinase Solyc11g033270 displayed a transient increase in normalized intensity. This correlated highest with a transient phosphorylation of a calmodulin domain containing protein (DYS(ph)ASGYSSR, solyc06g053530) and a transcriptional regulator (S(ph)PIPLEAVK, Solyc01g097890). However, while our data set reveals correlative relationships between the phosphorylation sites that may be indicative of enzyme-substrate interaction, it must be kept in mind that the data does not directly allow to derive the activity change of the respective proteins without further experiments.

Within this network, we then displayed the degree distribution of phosphopeptides from systemin-specific kinases/phosphatases, other kinases/phosphatases and the putative targets for systemin-induced clusters A to F (Figure 7C, D). It becomes apparent that systemin-specific kinases in clusters B, C, and D (which showed a transient phosphorylation increase) showed a higher degree than kinases without systemin specificity, but kinases in generally had higher degree than their target proteins (Figure 7C). In contrast, for phosphatases, higher than average degree was observed for nine systemin-specific phosphatases in cluster A (rapid dephosphorylation response). In cluster F (no systemin induced phosphorylation response), higher than average degree was observed for nine other phosphatases (those not linked to the systemin response). This observation supports the conclusion that the kinases identified as systemin-specific, are indeed responsible for the phosphorylation events that peak at 2 minutes (cluster B), 5 minutes (cluster C) and 15 minutes (cluster D) of stimulation, while systemin-specific phosphatases mediate rapid dephosphorylation responses (cluster A). A full list of kinase-target relationships is available in Supplementary Table 6. Selected candidate targets for systemin-specific kinases and phosphatases are addressed below.

Plasma membrane H^+-ATPases

Phosphopeptides matching two different plasma membrane H^+-ATPases showed systemin-induced correlation with phosphopeptides of distinct kinases and phosphatases (Figure 8A). Phosphopeptides of receptor kinases (Solyc02g079590, Solyc02g076780), MAP-kinase MPK2 (Solyc08g014420), a MAP-triple kinase (Solyc11g033270), were highly correlated to phosphopeptides encompassing the activating C-terminal phosphorylation site at T955 of LHA1 (GLDIETIQQSYT(ph)V, Solyc03g113400) and T964 of H^+-ATPase solyc07g017780 (GLDIETIQQHYT(ph)V, Solyc07g017780). We suggest that

these kinases may directly phosphorylate the respective residues in the H^+-ATPases. Thereby, kinases with highest correlation to well studied C-terminal activating phosphopeptide GLDIETIQQSYT(ph)V of LHA1 were receptor kinase Solyc02g079590 (r=0.99) and MPK2 (Solyc08g014420) (r=0.98). This C-terminal peptide peptide GLDIETIQQSYT(ph)V also was highly correlated with the homolog of Arabidopsis POLTERGEIST-LIKE 5 phosphatase (PLL5, Solyc06g076100), a member of the PP2C clade C phosphatases (47). Highest correlation with phosphopeptide GLDIETIQQHYT(ph)V of H^+-ATPase solyc07g017780 was found with receptor kinase Solyc11g011020 (r=0.94).

The interaction of the C-terminal peptide of H^+-ATPase LHA1 with candidate kinase MPK2 and candidate phosphatase PLL5 was investigated by *in vitro* activity assays (Figure 8 B-E). Recombinant MPK2 was expressed either in wild-type form (WT) or as a constitutively active mutant (CA) with D216G and E220A amino acid substitutions (39). Kinase activity, assayed as ATP consumption, was observed only in presence of GLDIETIQQSYTV peptide substrate, and was higher for CA compared to WT (Figure 8B). Increasing the substrate peptide concentration from 10 µM to 200 µM resulted in increasing kinase activity (Figure 8C). Phosphorylation of the C-terminal LHA1 peptide substrate at T955 by recombinant MPK2 was confirmed by mass spectrometric analysis (supplementary figure 1A,C). Recombinant PLL5 was able to dephosphorylate synthetic phosphopeptide GLDIETIQQSY(pT)V *in vitro* (Figure 8D). PLL5 activity, assayed as release of inorganic phosphate, was observed only in presence of the phosphopeptide substrate, and increased with increasing substrate concentration (Figure 8E). De-phosphorylation of the LHA1-derived phosphopeptide substrate by PLL5 phosphatase was confirmed by mass spectrometric analysis (supplementary figure 1B,C). Interestingly PLL5 phosphatase was identified in systemin-induced cluster A (rapid dephosphorylation), while MPK2 was identified in systemin-induced cluster D with maximum phosphorylation of peptide VTSETDFM(ox)T(ph)EY(ph)VVTR at 15 minutes. The identified phosphopeptide contained the typical MAP-Kinase activating motif (pT)E(pY). Thus, the phosphatase may well be involved in dephosphorylation of LHA1 at early systemin stimulation, while MPK2 is a candidate kinase for re-phosphorylation (Figure 5A) with concomintant increase in H+-ATPase activity (Figure 5C) at later time points (15 min) of systemin treatment.

Respiratory burst oxidases

Another protein with highly systemin-specific phosphorylation response was the respiratory burst oxidase. Phosphopeptides were identified for two isoforms of respiratory burst oxidases (DVFSEPS(ph)QTGR, Solyc03g117980; NLSQM(ox)LS(ph)QK, Solyc06g068680). Potential interacting kinases include receptor kinase (Solyc09g064270 and Solyc02g07000) and a CBL-interacting protein kinase (Solyc06g068450, r=0.90). Phosphorylation of the respiratory burst oxidase occurred at early time points (2 minutes) with a strong transient increase of phosphorylation for both peptides. No such transient increase in phosphorylation of the respiratory burst oxidase was observed under A17 treatment (Supplementary Figure 2A).

Processes at the cell wall

Among the target proteins with most significant systemin-induced phosphorylation responses were cellulose synthase proteins. Four phosphopeptides matching cellulose synthase like proteins (SSS(ph)RLNLSTR Solyc04g077470, SHS(ph)GLMR Solyc08g076320, SSS(ph)ESGLAELNK Solyc09g057640, GLIDSQSLSSS(ph)PVK Solyc09g075550) were identified as potential targets of systemin-specific kinases and phosphatases (Supplementary Figure 2B). Systemin-induced phosphorylation changes of cellulose synthase-like proteins were either rapid dephosphorylation (cluster A) or transient phosphorylation at 2 minutes (cluster B). The transient phosphorylation of an uncharacterized receptor kinase at 2 minutes (NNTS(ph)SVSPDSVTAK, solyc12g036330) showed strongest correlation with the transient phosphorylation of peptide S(ph)SEGDLTLLVDGKPK of

cellulose synthase-like protein solyc04g077470, while dephosphorylation of peptide GQLPS(ph)GQVVAVK matching an uncharacterized receptor-like cytoplasmic kinase (Solyc05g024290) showed strongest correlation with dephosphorylation of peptide GLIDSQSLSSS(ph)PVK of cellulose-synthase-like protein (Solyc09g075550). These two peptides also showed a high correlation to a POLTERGEIST-LIKE 1 phosphatase (Solyc08g077150, peptide FVS(ph)PSQSLR; r=0.92).

Vesicle trafficking and G-Protein signaling

In total, 52 kinases and 8 phosphatases were found with high correlations to phosphopeptides of vesicle trafficking proteins. While phosphopeptides of adaptins and syntaxins were rapidly dephosphorylated (cluster A), most phosphopeptides of vesicle-associated membrane proteins (VAMPs) were transiently phosphorylated at 2 minutes of systemin stimulation (cluster B). For example, phosphopeptide NS(ph)DDGYSSDSILR in cluster A matching a KEU-homolog (Solyc10g008490) showed strong correlation (r=0.99) to phosphopeptide VNS(ph)LVQLPR matching the catalytic subunit of a protein phosphatase (Solyc10g008490). Phosphopeptide VVYIS(ph)PHS(ph)SPGHSEDAFK of VAMP Solyc04g015130 with transient phosphorylation at 2 minutes showed high correlation with a protein phosphatase 2C Solyc07g053760 and protein kinase Solyc06g068920.

Several phosphopeptides of small GTPase proteins were also identified and these proteins may also have functions in vesicle budding and fusions. Most prominent members of this group included the ARF GTPase activator Solyc05g023750 and RAB GTPase activator Solyc12g009610. The phosphopeptide NS(ph)SELGSGLLSR of the ARF-GTPase activator was identified as being rapidly dephosphorylated (cluster A), while phosphopeptide TLS(ph)SLELPR of the RAB-GTPase activator Solyc12g009610 was transiently phosphorylated at 2 minutes of systemin treatment. Phosphopeptide AELS(ph)VNR of a RAB-GTPase Solyc09g098170 was transiently phosphorylated at 5 minutes. Phosphopeptide NS(ph)SELGSGLLSR correlated highest with phosphopeptide ALIGEGS(ph)YGR of receptor kinase Solyc12g098980, phosphopeptide TLS(ph)SLELPR showed highest correlation with receptor kinase Solyc07g056270. Phosphorylation of the RAB-GTPase Solyc09g098170 correlated highest with receptor kinase Solyc07g055130 and the protein phosphatase 2C Solyc05g055790.

Calcium-related responses

Four IQ-domain 13-containing proteins (FTLPAGAVS(ph)PR Solyc08g014280, EAS(ph)PKVT(ph)SPR Solyc01g108920, LSFPLTPSS(ph)TGSVK Solyc10g008490, FNSLS(ph)PR Solyc05g014760) were rapidly dephosphorylated upon systemin stimulation (cluster A). Phosphopeptides of CBL-interacting kinase (Solyc04g076810), CDPK (Solyc04g009800) and MAP-triple-kinases (Solyc12g088940, Solyc11g033270) as well as a phosphopeptide of phosphatases (Solyc10g008490 and Solyc01g067500) showed strong correlation with dephosphorylation of the IQ-domain 13-containing proteins. A phosphopeptide of calcium-ATPase Solyc02g064680 displayed a transient phosphorylation at 5 minutes (cluster C). Phosphopeptides of phosphatase 2C (solyc05g055790) and kinases Solyc07g055130 and Solyc01g094920 showed high correlation with the phosphorylation profile of the calcium ATPase.

Transcription factors

Phosphopeptides of several transcription and splicing factor families (bin 27) were over-represented with similar abundance in all systemin-response clusters (supplementary Table 2). The highest number of identified phosphopeptides and highest degree for this functional protein group in the network (37) was observed for the RNA-processing factor SERRATE (Solyc01g009090) with matching phosphopeptides S(ph)PPFPPYK and NRS(ph)PPHHPPGR. Phosphopeptide S(ph)PPFPPYK was

transiently phosphorylated at 2 minutes and showed best correlation to phosphorylation sites of kinases CTR1 (Solyc09g009090), a MAP-triple kinase (Solyc12g088940), and a CBL-interacting kinase (Solyc04g076810). Phosphopeptide NRS(ph)PPHHPPGR was transiently phosphorylated at 5 minutes of systemin treatment. Phosphorylation sites of receptor kinases Solyc02g023950 and Solyc09g072810, a CDK-related kinase Solyc10g078390 and a MAP-triple kinase Solyc11g033270 showed high correlation with that second SERRATE phosphorylation site.

Interactions with other phytohormone signaling pathways

Among the specifically systemin-induced phosphorylation/dephosphorylation events were several phosphopeptides of proteins known from other hormone signaling pathways. For example, phosphopeptides of abscisic acid (ABA) response factors (ASSESSSEDEADS(ph)AEEAGSSK, Solyc04g081340; VGS(ph)PGNDFIAR, Solyc01g108080), auxin response factor (INS(ph)PSNLR, Solyc05g047460), EIN4 (GGT(ph)PELVDTR, Solyc05g055070) and PIN3 (PSNFEENCAPGGLVQS(ph)SPR, Solyc05g008060) were rapidly dephosphorylated upon systemin treatment (cluster A). Another phosphorylation site in ABA-response factor Solyc04g081340 (RSS(ph)ASATQVQAEEQAPR), SSS(ph)RLNLSTR of ACC-synthase (Solyc03g007070), and another phosphopeptide of EIN4 (RSS(ph)ASATQVQAEEQAPR) were transiently phosphorylated at 2 minutes of systemin treatment. A third phosphopeptide of EIN4 (GGS(ph)QTDSSISTSHFGGK) was transiently phosphorylated at 5 minutes of systemin treatment. Kinases with high correlations to the phosphorylation patterns in cluster A were CTR1 (Solyc09g009090), a receptor kinase (Solyc11g011020), and a CBL-interacting protein kinase (Solyc04g076810).

Discussion

The aim of our work was to (i) identify early events induced by systemin and (ii) identify kinases and phosphatases involved in these signaling events. The maturation of the signaling peptide systemin is beginning to be understood (9), and the primary receptor of systemin was recently identified (16). While individual early responses to systemin perception, such as an increase in cytosolic calcium (17), ROS production (16, 48), the modulation of the H^+-ATPase activity (19), or the activation of MAP-kinase signaling (49) have been identified, the proteome-wide effects of systemin treatment were not yet studied.

The use of inactive analogon A17 to define systemin-specific responses

Antagonistic and inactive peptides—such as mutant peptide variants, chemically modified peptides or peptide mimetics, are important tools for the characterization of peptide-receptor interaction and to discover endogenous peptide function (50-52). For example, the dominant-negative effect produced by antagonistic peptides can be used for the characterization of peptide function when suitable mutants are not available, and in the case of genetic redundancy (53, 54). The use of inactive analoga in studying receptor signaling pathways provides an elegant way to define specific responses and rule-out common unspecific treatment responses. Comparing the responses to systemin and the antagonistic A17 analog, approximately half of the identified phosphopeptides could be identified as not specific to the systemin treatment and were excluded from the reconstruction of the systemin signaling network. Including the A17 analog thus allowed us to gain insight into systemin-specific protein signaling processes.

Systemin-induced modulation of the plasma membrane H+-ATPase

Systemin-induced alkalization of the growth medium has been well described (18, 19, 51). Alkalization of the growth medium is a typical process connected with inhibition of the plasma

membrane H^+-ATPase, as it also occurs upon stimulation by flagellin and other microbe-associated molecular patterns (31, 55, 56). By pairwise correlation of phosphopeptide abundance profiles we identified the H^+-ATPase LHA1 as putative target of 12 kinases and two phosphatases, while receptor like kinase Solyc11g011020 was the only kinase putatively involved in the phosphorylation of LHA1. These kinase-substrate predictions were confirmed by *in-vitro* kinase and phosphatase assays. MPK2 and PLL5 phosphatase were found to indeed act on the respective peptide of LHA1. While such verification can only be done for a limited number of kinases or phosphatases, the results obtained for MPK2 and PLL5 phosphatase confirm the general validity of our correlation analysis. We thus consider the correlation analysis for prediction of kinase/phosphatase-substrate interactions as a powerful means to predict new regulatory circuits in the systemin signaling network. Thereby we identified a novel connection of the MPK pathway with the plasma membrane H^+-ATPase LHA1. MPK2 is activated by phosphorylation of the typical TEY motif at 15 minutes of systemin treatment and, therefore, is a primary candidate for re-phosphorylation of the H^+-ATPase at later times of systemin stimulation. Phosphorylation by MPK2 occurred at the penultimate regulatory threonine residue resulting in activation of the proton pump. MPK2-mediated activation of LHA1 is thus likely to be responsible for re-acidification of the extracellular space dampening the initial alkalization response.

While knowledge of specific interactions of phosphatases with their substrates is still limited in plants, several phosphatases have been implicated in the regulation of the plasma membrane proton pump. This includes a type 2A phosphatase activity partially purified from maize roots (57), an unidentified type 2C phosphatase in Arabidopsis seedlings and *Vicia faba* guard cells (58), and PP2C clade D phosphatases that are involved in proton pump regulation during auxin-induced acid growth of Arabidopsis hypocotyls (59). PP2C-D3 (alias PP2C38; At4g28400) also was shown to dephosphorylate BIK1 attenuating immune signaling through the FLS2 and EFR pattern recognition receptors (60). Likewise, EFR-mediated signaling also is downregulated by Arabidopsis PLL4 and PLL5 phosphatases, which belong to PP2C clade C (61). We show here that the tomato PLL5 homolog, is (i) involved in systemin signaling and (ii) dephosphorylates LHA1. The precise mechanisms of PP2C phosphatase regulation and signaling are still unclear, especially if and how they are activated or inactivated by reversible phosphorylation (62). Under the assumption that similar to PP2A proteins (62), PLL5 phosphatase may be activated by de-phosphorylation (consistent with its identification in systemin-induced cluster A), it is a primary candidate for proteins involved in the downregulation of H^+-ATPase activity and the resulting alkalization of the growth medium.

Reconstruction of early vs. late responses from plasma membrane to the nucleus

The recently identified plasma membrane located LRR-RLK receptors for the systemin peptide were not identified among the 3312 phosphopeptides from this work, while several other receptor kinases, among them also the phytosulfokine receptor PSKR2 (Solyc07g063000) or FERONIA (Solyc09g015830) were quantified in our experiments. Possibly, some important receptor kinases were not enriched in the membrane purification protocol due to their strong embedding within the cell wall. Nonetheless, our work identified 57 systemin specific kinases and 18 phosphatases to be involved in systemin signaling, likely downstream of the primary systemin receptor SYR1 (16). Substrates for these kinases and phosphatases were identified by pairwise correlations. Correlation analysis was previously used to reconstruct topology of phosphorylation networks induced by external nutrient supply (63). Thereby, plasma membrane proteins were identified as signal induction layers within the network, while cytosolic and nuclear proteins were considered as an effector layer.

Considering the absence of phosphopeptides from recently identified systemin receptors, the earliest harvesting time point of 2 minutes may have been already too late to capture the immediate first

systemin responses. Ligand-induced phosphorylation of ligand-perceiving receptor kinases is known to occur within seconds (64). The identified phosphorylation patterns at 2 minutes may thus represent early responses of the systemin signaling cascade. This point of view is supported by the observation of rapid (de)phosphorylation changes for several cytosolic proteins such as a CBL-interacting kinase, MAP-triple kinase, and CDPKs already at 2 minutes (clusters A and B), while a large number of receptor kinases with systemin specific phosphorylation patterns peak only after 5 minutes. Also observed very rapidly after systemin stimulation are plasma membrane-located proteins that are known to belong to the systemin signaling cascade, including the proton pump that is rapidly de-phosphorylated after systemin treatment, and two RBOHD isoforms showing a strong increase of phosphorylation after 2 minutes, compared to G-protein signaling or transcription factor phosphorylation at later times.

Conclusions

Our study presents 56 systemin specific kinases and 18 systemin specific phosphatases. Putative substrates were identified by pairwise correlations of systemin induced phosphorylation time profiles. Thereby we identified novel candidates for the systemin signaling pathway. Two of these candidates, MPK2 and PLL5 were confirmed as kinase and phosphatase for reversible phosphorylation of the C-terminal regulatory site of the plasma membrane H^+-ATPase. We highlighted several proteomic processes upon systemin stimulation ranging from plasma membrane processes to cytosolic and nuclear signaling, which will provide a valuable resource for further in-depth functional studies in future elucidation of systemin signaling cascades.

Acknowledgements

The work was supported by a grant from the Deutsche Forschungsgemeinschaft SFB 1101/D06 to Andreas Schaller. We thank Ursula Glück -Behrens for maintenance of the *S. peruvianumicotiana* Benthamiana cell culture and Denise Llanos Jara for excellent assistance during sample preparation and mass spectrometry.

References

1. Pearce, G., Strydom, D., Johnson, S., and Ryan, C. A. (1991) A polypeptide from tomato leaves induces wound-inducible proteinase inhibitor proteins. *Science* 253, 895-897
2. Ryan, C. A., and Pearce, G. (1998) Systemin: A polypeptide signal for plant defensive genes. *Annual Review of Cell and Developmental Biology* 14, 1-17
3. McGurl, B., Orozco-Cardenas, M., Pearce, G., and Ryan, C. A. (1994) Overexpression of the prosystemin gene in transgenic tomato plants generates a systemic signal that constitutively induces proteinase inhibitor synthesis. *Proc. Natl. Acad. Sci. U S A* 91, 9799-9802
4. McGurl, B., Pearce, G., Orozco-Cardenas, M., and Ryan, C. A. (1992) Structure, expression and antisense inhibition of the systemin precursor gene. *Science* 255, 1570-1573
5. Schaller, A., and Ryan, C. A. (1996) Systemin – a polypeptide defense signal in plants. *BioEssays* 18, 27-33
6. Ryan, C. A., and Moura, D. S. (2002) Systemic wound signaling in plants: a new perception. *Proc. Natl. Acad. Sci. U S A* 99, 6519-6520
7. Howe, G. A., and Schaller, A. (2008) Direct defenses in plants and their induction by wounding and insect herbivores. In: Schaller, A., ed. *Induced plant resistance against herbivory*, pp. 7-29, Springer, Heidelberg

8. Gust, A. A., Pruitt, R., and Nürnberger, T. (2017) Sensing danger: key to activating plant immunity. *Trends Plant Sci.*
9. Beloshistov, R. E., Dreizler, K., Galiullina, R. A., Tuzhikov, A. I., Serebryakova, M. V., Reichardt, S., Shaw, J., Taliansky, M. E., Pfannstiel, J., Chichkova, N. V., Stintzi, A., Schaller, A., and Vartapetian, A. B. (2018) Phytaspase-mediated precursor processing and maturation of the wound hormone systemin. *The New phytologist* 218, 1167-1178
10. Meindl, T., Boller, T., and Felix, G. (1998) The plant wound hormone systemin binds with the N-terminal part to its receptor but needs the C-terminal part to activate it. *Plant Cell* 10, 1561-1570
11. Scheer, J. M., and Ryan, C. A. (1999) A 160 kDa systemin receptor on the cell surface of *Lycopersicon peruvianum* suspension cultured cells: kinetic analyses, induction by methyl jasmonate and photoaffinity labeling. *Plant Cell* 11, 1525-1535
12. Scheer, J. M., and Ryan, C. A. (2002) The systemin receptor SR160 from *Lycopersicon peruvianum* is a member of the LRR receptor kinase family. *Proc. Natl. Acad. Sci. USA* 99, 9585–9590
13. Lanfermeijer, F. C., Staal, M., Malinowski, R., Stratmann, J. W., and Elzenga, J. T. M. (2008) Micro-electrode flux estimation confirms that the *Solanum pimpinellifolium cu3* mutant still responds to systemin. *Plant Physiol.* 146, 129-139
14. Hind, S., Malinowski, R., Yalamanchili, R., and Stratmann, J. W. (2010) Tissue-type specific systemin perception and the elusive systemin receptor. *Plant Signal. Behav.* 5, 42-44
15. Montoya, T., Nomura, T., Farrar, K., Kaneta, T., Yokota, T., and Bishop, G. J. (2002) Cloning the tomato Curl3 gene highlights the putative dual role of the leucine-rich repeat receptor kinase tBRI1/SR160 in plant steroid hormone and peptide hormone signaling. *Plant Cell* 14, 3163-3176
16. Wang, L., Einig, E., Almeida-Trapp, M., Albert, M., Fliegmann, J., Mithofer, A., Kalbacher, H., and Felix, G. (2018) The systemin receptor SYR1 enhances resistance of tomato against herbivorous insects. *Nat Plants* 4, 152-156
17. Moyen, C., Hammond-Kosack, K. E., Jones, J., Knight, M. R., and Johannes, E. (1998) Systemin triggers an increase of cytoplasmic calcium in tomato mesophyll cells: Ca^{2+} mobilization from intra- and extracellular compartments. *Plant Cell Environ.* 21, 1101-1111
18. Felix, G., and Boller, T. (1995) Systemin induces rapid ion fluxes and ethylene biosynthesis in *Lycopersicon peruvianum* cells. *Plant J.* 7, 381-389
19. Schaller, A., and Oecking, C. (1999) Modulation of plasma membrane H+-ATPase activity differentially activates wound and pathogen defense responses in tomato plants. *Plant Cell* 11, 263-272
20. Farmer, E. E., and Ryan, C. A. (1992) Octadecanoid-derived signals in plants. *Trends Cell Biol.* 2, 236-241
21. Wasternack, C., and Hause, B. (2013) Jasmonates: biosynthesis, perception, signal transduction and action in plant stress response, growth and development. An update to the 2007 review in Annals of Botany. *Ann. Bot.* 111, 1021-1058
22. Schaller, A., and Stintzi, A. (2008) Jasmonate biosynthesis and signaling for induced plant defense against herbivory. In: Schaller, A., ed. *Induced plant resistance against herbivory*, pp. 349-365, Springer, Heidelberg
23. Schilmiller, A. L., and Howe, G. A. (2005) Systemic signaling in the wound response. *Current opinion in plant biology* 8, 369-377
24. Mousavi, S. A. R., Chauvin, A., Pascaud, F., Kellenberger, S., and Farmer, E. E. (2013) GLUTAMATE RECEPTOR-LIKE genes mediate leaf-to-leaf wound signalling. *Nature* 500, 422-426
25. Toyota, M., Spencer, D., Sawai-Toyota, S., Jiaqi, W., Zhang, T., Koo, A. J., Howe, G. A., and Gilroy, S. (2018) Glutamate triggers long-distance, calcium-based plant defense signaling. *Science* 361, 1112-1115
26. Wildon, D. C., Thain, J. F., Minchin, P. E. H., Gubb, I. R., Reilly, A. J., Skipper, Y. D., Doherty, H. M., O'Donnell, P. J., and Bowles, D. J. (1992) Electrical signalling and systemic proteinase inhibitor induction in the wounded plant. *Nature* 360, 62-65
27. Niittylä, T., Fuglsang, A. T., Palmgren, M. G., Frommer, W. B., and Schulze, W. X. (2007) Temporal analysis of sucrose-induced phosphorylation changes in plasma membrane proteins of Arabidopsis. *Mol. Cell. Proteomics* 6, 1711-1726

28. Wu, X., Sanchez-Rodriguez, C., Pertl-Obermeyer, H., Obermeyer, G., and Schulze, W. X. (2013) Sucrose-induced receptor kinase SIRK1 regulates a plasma membrane aquaporin in Arabidopsis. *Mol. Cell. Proteomics* 12, 2856-2873
29. Wang, X., Bian, Y., Cheng, K., Zou, H., Sun, S. S., and He, J. X. (2012) A comprehensive differential proteomic study of nitrate deprivation in Arabidopsis reveals complex regulatory networks of plant nitrogen responses. *J. Proteome Res.* 11, 2301-2315
30. Lin, L. L., Hsu, C. L., Hu, C. W., Ko, S. Y., Hsieh, H. L., Huang, H. C., and Juan, H. F. (2015) Integrating Phosphoproteomics and Bioinformatics to Study Brassinosteroid-Regulated Phosphorylation Dynamics in Arabidopsis. *BMC Genomics* 16, 533
31. Haruta, M., Sabat, G., Stecker, K., Minkoff, B. B., and Sussman, M. R. (2014) A peptide hormone and its receptor protein kinase regulates plant cell expansion. *Science* 343, 408-411
32. Nitsch, J. P., and Nitsch, C. (1969) Haploid plants from pollen grains. *Science* 163, 85-87
33. Wu, X. N., Xi, L., Pertl-Obermeyer, H., Li, Z., Chu, L. C., and Schulze, W. X. (2017) Highly Efficient Single-Step Enrichment of Low Abundance Phosphopeptides from Plant Membrane Preparations. *Front Plant Sci* 8, 1673
34. Larsen, M. R., Thingholm, T. E., Jensen, O. N., Roepstorff, P., and Jorgensen, T. J. D. (2005) Highly selective enrichtment of phosphorylated peptides from peptide mixtures using titanium dioxide microcolumns. *Mol. Cell. Proteomics* 4, 873-886
35. Rappsilber, J., Ishihama, Y., and Mann, M. (2003) Stop And Go Extraction tips for matrix-assisted laser desorption/ionization, nanoelectrospray, and LC/MS sample pretreatment in proteomics. *Anal. Chem.* 75, 663-670
36. Cox, J., and Mann, M. (2008) MaxQuant enables high peptide identification rates, individualized p.p.b.-range mass accuracies and proteome-wide protein quantification. *Nature Biotechnol.* 26, 1367-1372
37. Cox, J., Neuhauser, N., Michalski, A., Scheltema, R. A., Olsen, J. V., and Mann, M. (2011) Andromeda: a peptide search engine integrated into the MaxQuant environment. *J. Proteome Res.* 10, 1794-1805
38. Zauber, H., and Schulze, W. X. (2012) Proteomics wants cRacker: Automated standardized data analysis of LC/MS derived proteomic data. *J. Proteome Res.* 11, 5548-5555
39. Genot, B., Lang, J., Berriri, S., Garmier, M., Gilard, F., Pateyron, S., Haustraete, K., Van Der Straeten, D., Hirt, H., and Colcombet, J. (2017) Constitutively Active Arabidopsis MAP Kinase 3 Triggers Defense Responses Involving Salicylic Acid and SUMM2 Resistance Protein. *Plant Physiol* 174, 1238-1249
40. He, Z., and Honeycutt, C. W. (2005) A modified molybdenum blue method for orthophosphate determination suitable for investigating enzymatic hydrolysis of organic phosphates. *Communications in Soil Science and Plant Analysis* 36, 1373-1383
41. Moyen, C., and Johannes, E. (1996) Systemin transiently depolarizes the tomato mesophyll cell membrane and antagonizes fusicoccin-induced extracellular acidification of mesophyll tissue. *Plant Cell Environ.* 19, 464-470
42. Schaller, A., and Frasson, D. (2001) Induction of wound response gene expression in tomato leaves by ionophores. *Planta* 212, 431-435
43. Pearce, G., Johnson, S., and Ryan, C. A. (1993) Structure-activity of deleted and substituted systemin, an 18-amino acid polypeptide inducer of plant defensive genes. *J. Biol. Chem.* 268, 212-216
44. Schaller, A., Bergey, D. R., and Ryan, C. A. (1995) Induction of wound response genes in tomato leaves by bestatin, an inhibitor of aminopeptidases. *Plant Cell* 7, 1893-1898
45. Svennelid, F., Olsson, A., Piotrowski, M., Rosenquist, M., Ottman, C., Larsson, C., Öcking, C., and Sommarin, M. (1999) Phosphorylation of Thr-948 at the C terminus of the plasma membrane H(+)-ATPase creates a binding site for the regulatory 14-3-3 protein. *Plant Cell* 11, 2379-2391
46. Fuglsang, A. T., Visconti, S., Drumm, K., Jahn, T., Stensballe, A., Mattei, B., Jensen, O. N., Aducci, P., and Palmgren, M. G. (1999) Binding of 14-3-3 protein to the plasma membrane H(+)-ATPase AHA2 involves the three C-terminal residues Tyr(946)-Thr-Val and requires phosphorylation of Thr(947). *J. Biol. Chem.* 274, 36774-36780

47. Fuchs, S., Grill, E., Meskiene, I., and Schweighofer, A. (2013) Type 2C protein phosphatases in plants. *FEBS J* 280, 681-693
48. Orozco-Cardenas, M., and Ryan, C. A. (1999) Hydrogen peroxide is generated systemically in plant leaves by wounding and systemin via the octadecanoid pathway. *Proceedings of the National Academy of Sciences of the United States of America* 96, 6553-6557
49. Kandoth, P. K., Ranf, S., Pancholi, S. S., Jayanty, S., Walla, M. D., Miller, W., Howe, G. A., Lincoln, D. E., and Stratmann, J. W. (2007) Tomato MAPKs LeMPK1, LeMPK2, and LeMPK3 function in the systemin-mediated defense response against herbivorous insects. *Proceedings of the National Academy of Sciences of the United States of America* 104, 12205-12210
50. Czyzewicz, N., Wildhagen, M., Cattaneo, P., Stahl, Y., Pinto, K. G., Aalen, R. B., Butenko, M. A., Simon, R., Hardtke, C. S., and De Smet, I. (2015) Antagonistic peptide technology for functional dissection of CLE peptides revisited. *J. Exp. Bot.* 66, 5367-5374
51. Schaller, A. (1998) Action of proteolysis-resistant systemin analogues in wound signalling. *Phytochemistry* 47, 605-612
52. Schardon, K., Hohl, M., Graff, L., Pfannstiel, J., Schulze, W., Stintzi, A., and Schaller, A. (2016) Precursor processing for plant peptide hormone maturation by subtilisin-like serine proteinases. *Science* 354, 1594-1597
53. Song, X. F., Guo, P., Ren, S. C., Xu, T. T., and Liu, C. M. (2013) Antagonistic peptide technology for functional dissection of CLV3/ESR genes in arabidopsis. *Plant Physiol.* 161, 1076-1085
54. Xu, T.-T., Ren, S.-C., Song, X.-F., and Liu, C.-M. (2015) CLE19 expressed in the embryo regulates both cotyledon establishment and endosperm development in Arabidopsis. *J. Exp. Bot.* 66, 5217-5227
55. Nühse, T. S., Bottrill, A. R., Jones, A. M., and Peck, S. C. (2007) Quantitative phosphoproteomic analysis of plasma membrane proteins reveals regulatory mechanisms of plant innate immune responses. *Plant J.* 51, 931-940
56. Boller, T., and Felix, G. (2009) A renaissance of elicitors: Perception of microbe-associated molecular patterns and danger signals by pattern-recognition receptors. *Annual Review of Plant Biology*, pp. 379-407
57. Camoni, L., Iori, V., Marra, M., and Aducci, P. (2000) Phosphorylation-dependent interaction between plant plasma membrane H(+)ATPase and 14-3-3 proteins. *J. Biol. Chem.* 275, 99919-99923
58. Hayashi, Y., Nakamura, S., Takemiya, A., Takahashi, Y., Shimazaki, K., and Kinoshita, T. (2010) Biochemical characterization of in vitro phosphorylation and dephosphorylation of the plasma membrane H+-ATPase. *Plant Cell Physiol* 51, 1186-1196
59. Spartz, A. K., Ren, H., Park, M. Y., Grandt, K. N., Lee, S. H., Murphy, A. S., Sussman, M. R., Overvoorde, P. J., and Gray, W. M. (2014) SAUR Inhibition of PP2C-D phosphatases activates plasma membrane H^+-ATPases to promote cell expansion in Arabidopsis. *Plant Cell* 26, 2129-2142
60. Couto, D., Niebergall, R., Liang, X., Bücherl, C. A., Sklenar, J., Macho, A. P., Ntoukakis, V., Derbyshire, P., Altenbach, D., Maclean, D., Robatzek, S., Uhrig, J., Menke, F., Zhou, J.-M., and Zipfel, C. (2016) The Arabidopsis Protein Phosphatase PP2C38 negatively regulates the central immune kinase BIK1. *PLoS Pathog.* 12, e1005811
61. Holton, N., Nekrasov, V., Ronald, P. C., and Zipfel, C. (2015) The phylogenetically-related pattern recognition receptors EFR and XA21 recruit similar immune signaling components in monocots and dicots. *PLoS Pathog.* 11, e1004602
62. Shi, Y. (2009) Serine/threonine phosphatases: mechanism through structure. *Cell* 139, 468-484
63. Duan, G., Walther, D., and Schulze, W. X. (2013) Reconstruction and analysis of nutrient-induced phosphorylation networks in Arabidopsis thaliana. *Frontiers in Plant Science* 4, 540
64. Schulze, B., Mentzel, T., Jehle, A. K., Müller, K., Beeler, S., Boller, T., Felix, G., and Chinchilla, D. (2010) Rapid heteromerization and phosphorylation of ligand-activated plant transmembrane receptors and their associated kinase BAK1. *J. Biol. Chem.* 285, 9444-9451

Figures

Figure 1: Analysis of the systemin signaling response. (**A**) Experimental design and analytical workflow. (**B**) Frequency distributions of 3312 identified phosphopeptides according to numbers of phosphorylation sites and phosphorylated amino acid as determined by MaxQuant. (**C**) Frequency of phosphosites per peptide as determined by MaxQuant.

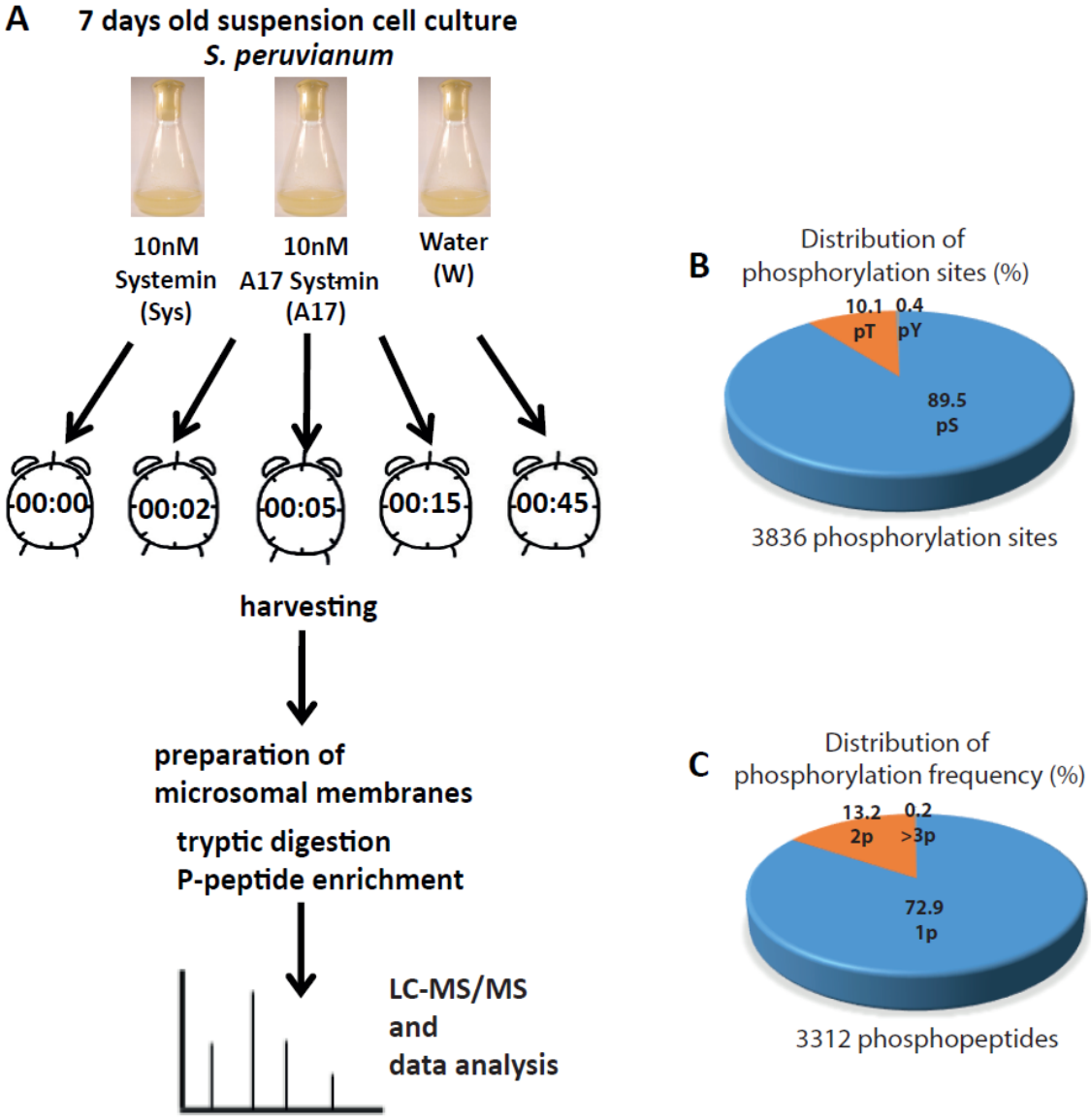

Figure 2: Alkalization response. (**A**) Time course of pH change after systemin treatment (blue) and A17 treatment (red) as well as competition of systemin response with increasing concentrations of A17 (blue to red). (**B**) Inhibition curve of A17. Data points show the mean with standard deviation from three independent experiments.

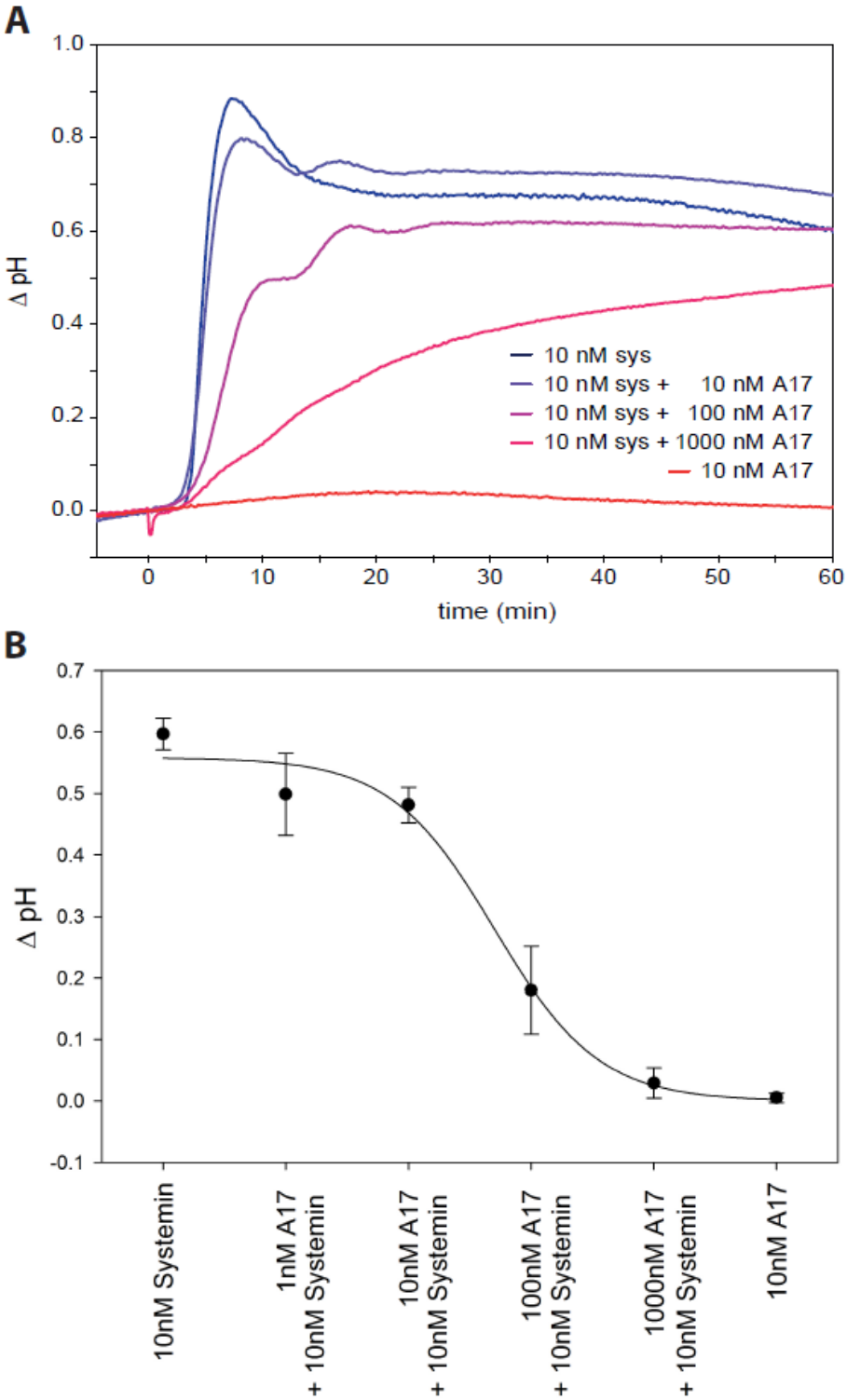

Figure 3: Overview of identified phosphorylation sites. (**A**) All phosphopeptides identified after systemin treatment at different time points. (**B**) Overlap of phosphopeptides identified after treatment with systemin, A17, or water at different time points.

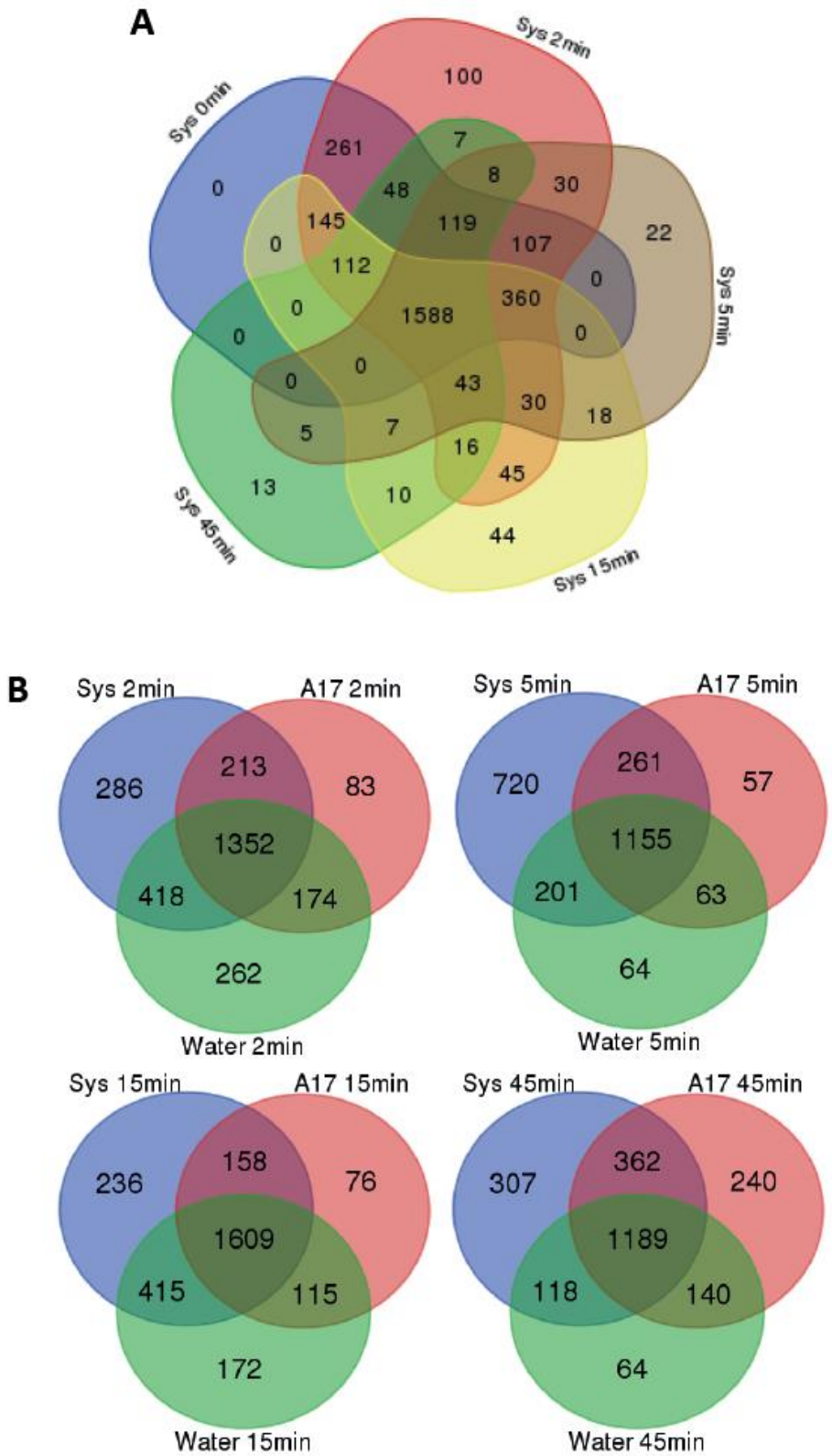

Figure 4: k-Means clustering of phosphorylation time courses. (**A**) Systemin treatment. (**B**) A17 treatment. (**C**) Water treatment. Numbers of identified phosphopeptides are indicated within each panel.

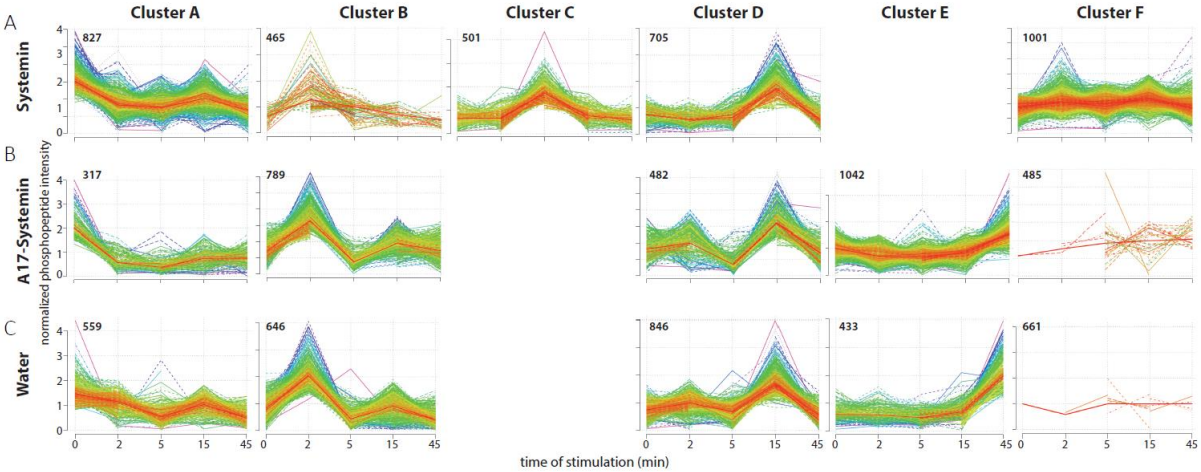

Figure 5: Phosphorylation of H^+-ATPase and respiratory burst oxidase. (**A**) C-terminal activating phosphorylation site of H^+-ATPase Solyc03g113400. (**B**) C-terminal activating phosphorylation site of H^+-ATPase Solyc07g017780. (**C**) H^+-ATPase activity under treatment with systemin, A17, and water. Black triangles: systemin treatment; white triangles: A17 treatment. White circles: water treatment. Mean values of three biological replicates are shown with standard deviation.

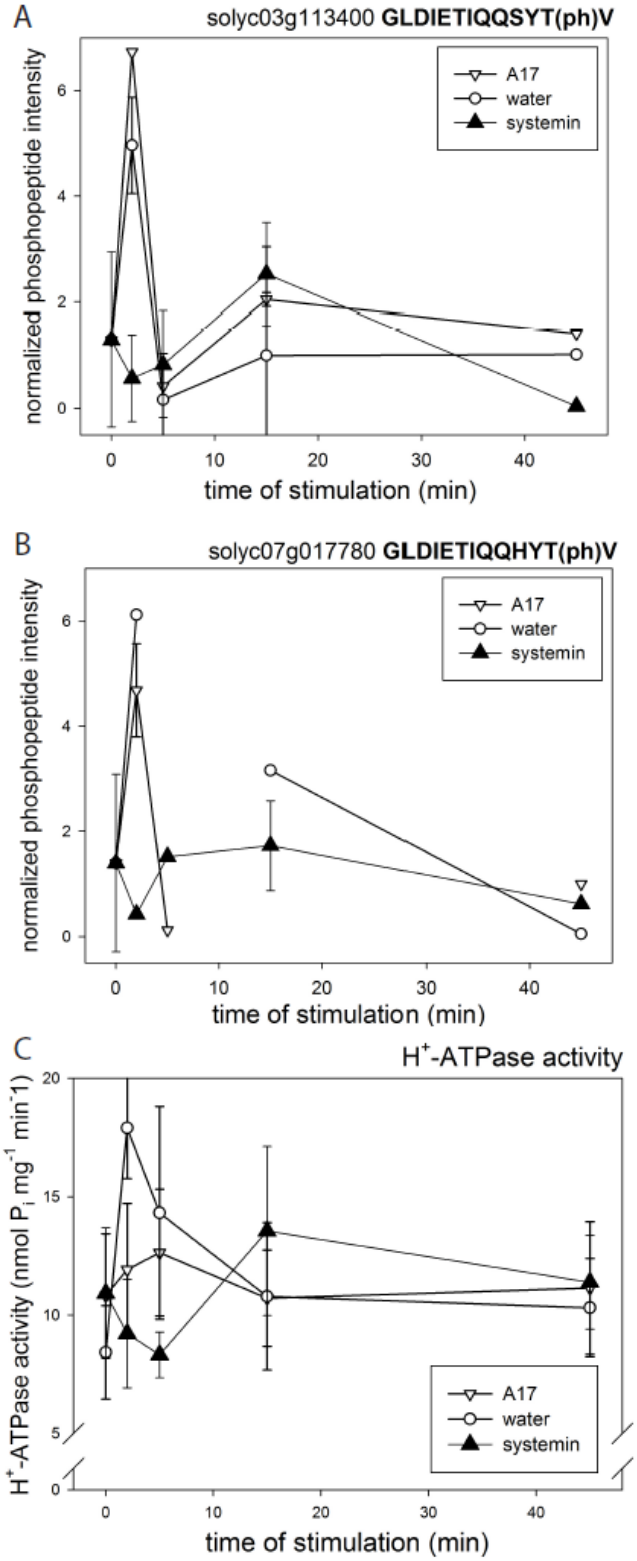

Figure 6: Over-representation analysis of functional groups in each cluster. (**A**) Network view of processes over-represented at different time points. Yellow colored "time"-nodes represent k-means clusters (figure 4) with maximum phosphorylation at respective time points. The "bin"-nodes represent the processes over-represented in the respective k-means clusters. Edges width represents the percentage of proteins of each bin within in each k-means cluster. Edge color indicates the processes involved at different time points. (**B**) Comparison of systemin and A17 response. The proportion of phosphopeptides with a time-shifted response in A17 treatment compared to systemin treatment is displayed. "Late" peptides display a later phosphorylation maximum at A17 treatment compared to systemin treatment, or do not display any maximum at all. "Early" peptides have a phosphorylation maximum at earlier time points after A17 treatment compared to systemin stimulation, or they have a maximum in A17 treatment and remain unaltered under systemin treatment. Numbers indicate absolute numbers of classified phosphopeptides.

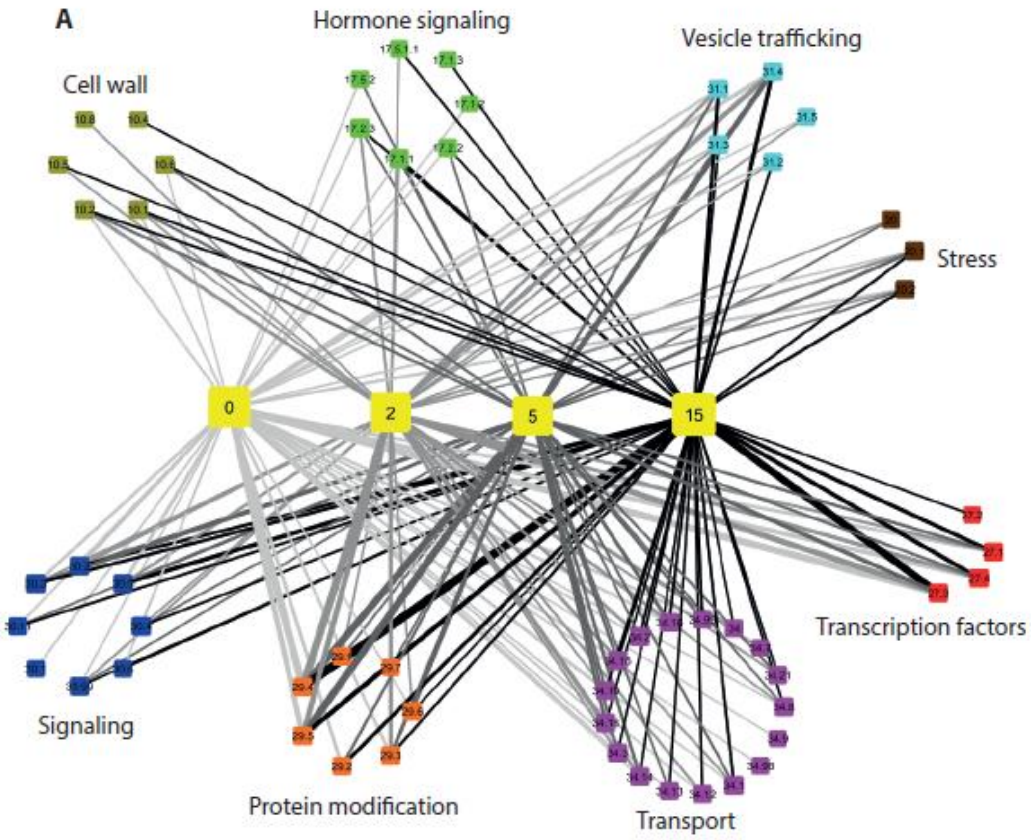

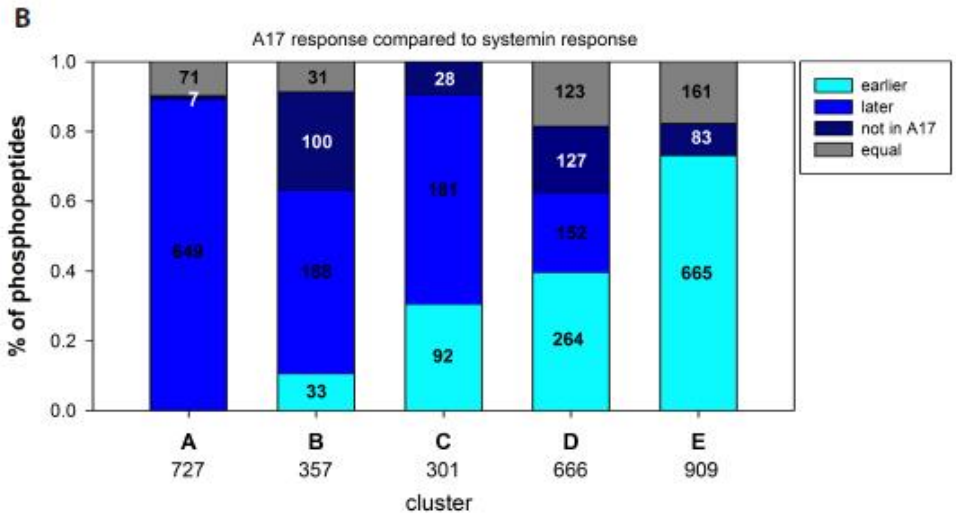

Figure 7: Correlation network of systemin specific kinases and phosphatases. (**A**) Kinase network. (**B**) Phosphatase network. Central nodes are the 57 kinases or 18 phosphatases, peripheral nodes represent individual proteins summarized under MapMan subbins. Node size is proportional to the degree, edge width is proportional to the correlation r-value (cutoff r=0.85). (**C**) Degree distribution of systemin-specific kinases, other kinases and their targets in different systemin response clusters. (**D**) Degree distribution of systemin-specific phosphatases, other phosphatases and their targets in different systemin response clusters. Values represent mean with standard error. For each class, the number of proteins is indicated.

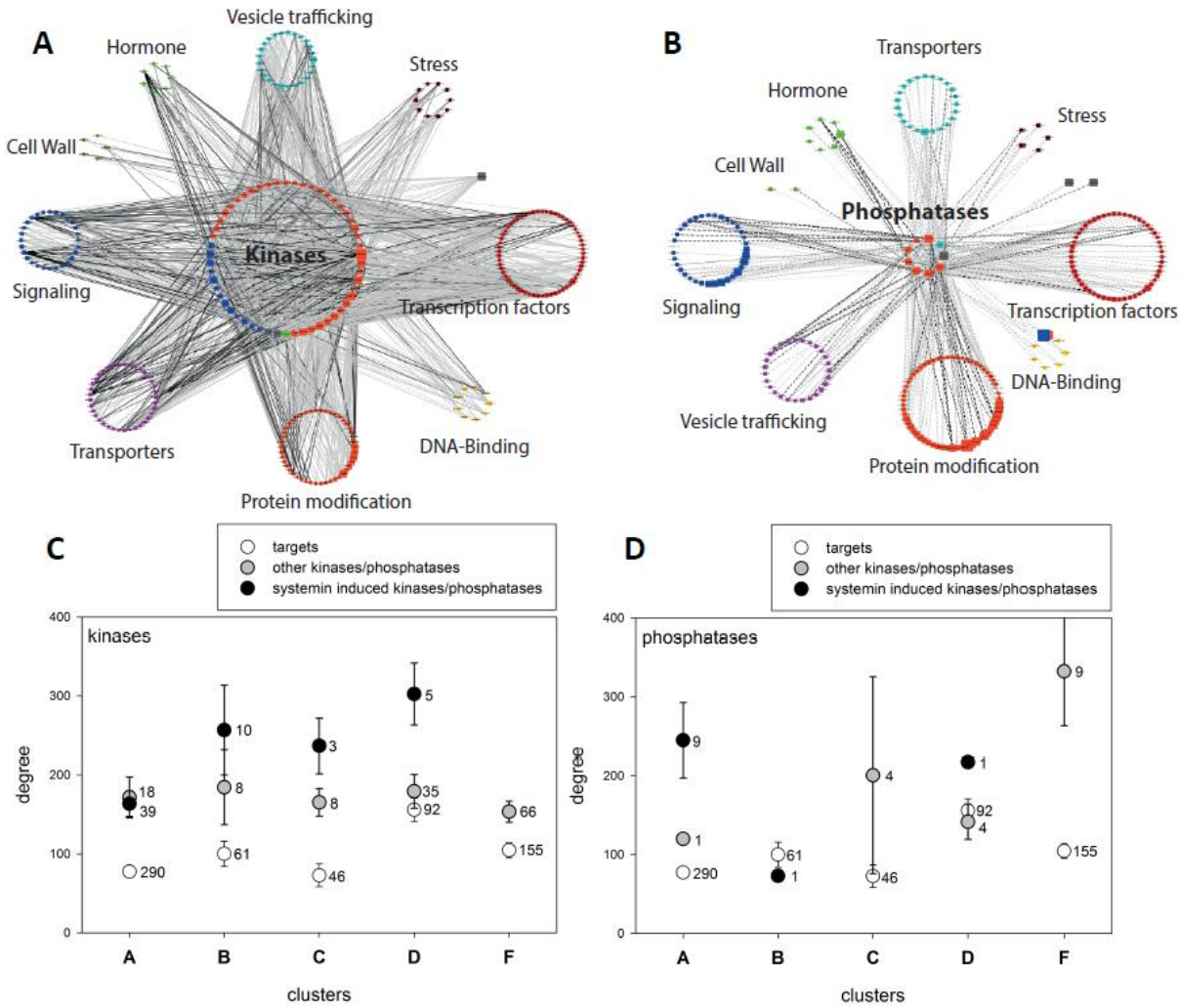

Figure 8: Kinase/phosphatase relationships with major targets. (**A**) H^+-ATPases AHA1 and LHA1. Solid edges represent kinase-substrate relationships, dashed edges represent phosphatase-kinase relationships. Node size indicates the degree in the overall network (Figure 7), Node color represents Mapman function. Blue: receptor kinase (30.2), cyan: Phosphatases, red: calcium-dependent protein kinases, orange: protein.posttranslational modification (29.4), gray: unclassified function. (35). (**B**) ATP remaining after kinase MPK2 reaction using H^+-ATPase peptide GLDIETIQQSYTV as a substrate. (**C**) ATP remaining after MPK2 reaction with increasing concentrations of substrate peptide (**D**) Phosphate produced by Phosphatase PLL5 in the reaction with H^+-ATPase phosphopeptide GLDIETIQQSY(pT)V as a substrate. (**E**) Phosphate produced by PLL5 reaction with increasing concentrations of substrate peptides. Data represent the mean with standard deviation. Activity assays were carried out on two independent protein isolations in two technical replicates.

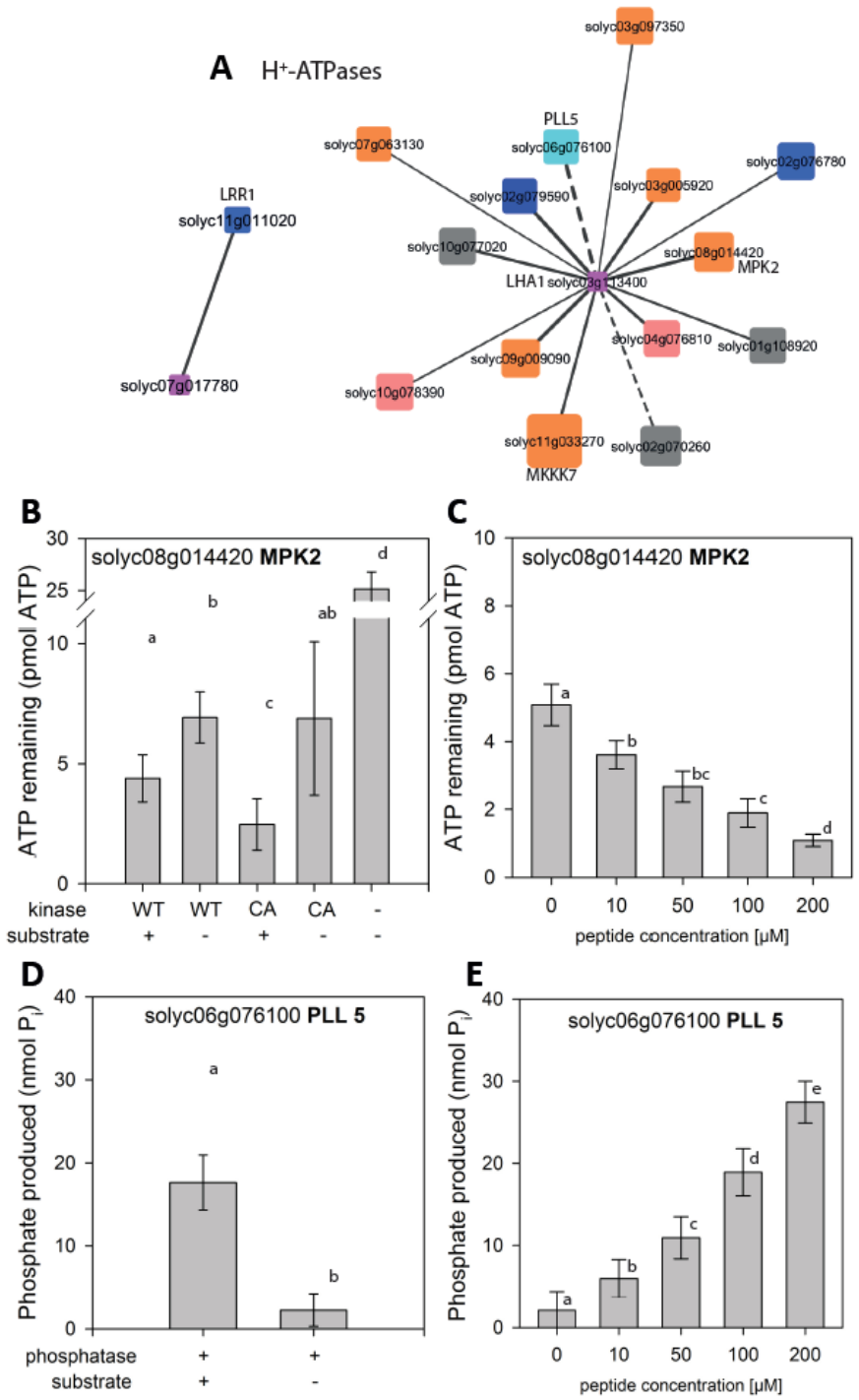

Supplementary Material

Supplementary Figure 1. Mass spectrometry analysis of in-vitro kinase and phosphatase assays. (**A**) Representative spectrum of kinase reaction with recombinant MPK2 resulting in phosphopeptide GLDIETIQQSY(pT)V. (**B**) Representative spectrum of phosphatase reaction with recombinant PLL5 phosphatase resulting in dephosphorylated peptide GLDIETIQQSYTV. (**C**) Summary of ion intensities of phosphorylated and dephosphorylated C-terminal peptide of H+-ATPase LHA1. Input peptides are shown as bars without patterns, reaction results are indicated as hatched bars. Averages with standard deviations of two biological replicates from two independent recombinant protein preparations are shown.

Supplementary Figure 2. Kinase and phosphatase relationship with proteins from respiratory burst oxidase and cell wall proteins. (**A**) Respiratory Burst Oxidases. (**B**) Cellulose synthase like proteins. Edge color represents the time cluster of this interaction, light color indicates earlier clusters (2min), dark color indicates later clusters (15min). Solid edges represent kinase-substrate relationships, dashed edges represent phosphatase-kinase relationships. Node size indicates the degree in the overall network (Figure 7), Node color represents MapMan function. Blue: receptor kinase (30.2), cyan: phosphatases, orange: protein.posttranslational modification (29.4), gray: unclassified function. (35)

Supplementary Table 1: list of normalized ion intensities of quantified phosphopeptides under systemin, A17 and water treatment. Quantitative values were obtained by cRracker analysis (38). Average normalized intensities, standard deviations and number of spectra are shown.

Supplementary Table 2: k-means clusters of identified phosphopeptides for systemin, A17 and water treatment.

Supplementary Table 3: Over-representation anlaysis for all clusters upon systemin stimulation and tabular overview of the abundance distribution of proteins in subcategories to statistically significant over-represented MapMan bins. Numbers represent the distribution of proteins in each subbin across clusters (in %).

Supplementary Table 4: Distribution of functional categories with significant over-representation under systemin induction compared to different response categories under A17 treatment. All peptides were classified as being “not identified under A17”, “with later or earlier response in A17, or with equal response in A17. Numbers represent the distribution of proteins in each subbin across classifications (in %).

Supplementary Table 5: List of kinases and phosphatases considered as systemin-specific based on their phosphorylation profiles under systemin stimulation in comparison with A17 and water treatment.

Supplementary Table 6: Correlation network of systemin specific kinases and phosphatases and their targets based on pairwise correlation analysis of phosphopeptide time profiles.